NUMERICAL ANALYSIS OF WIDE PLATE TESTS AND ITS APPLICATION FOR FAILURE PREDICTIONS USING FEM

R. Twickler, M. Twickler and W. Dahl*

The results of two- and three-dimensional finite element calculations of a double edge notched wide plate are discussed in terms of loads, integral displacements and J-integral values. Comparisons between finite element calculations and experiments over a wide temperature range are presented in terms of general-yield stresses, thereby studying the influence of the choice of the yield criterion and the influence of the strain rate. Finally the results are used for a failure assessment of wide plates with special view of investigating the influence of the geometry dependence of fracture mechanics properties on predicted failure loads and on the predicted characteristic transition temperature T_{gy}.

INTRODUCTION

In order to assess the failure of structural components containing cracks several concepts based on fracture mechanics as e.g. the engineering approach for elastic-plastic fracture analysis by Kumar et al. (1) have been developed. Within these concepts the quantitative estimation of failure loads requires an exact evaluation of the material properties (yielding behaviour, fracture mechanics properties) and a precise determination of the loading conditions in terms of a fracture mechanics parameter as e.g. K_I, J_I or CTOD. If the transferability of such a fracture mechanics property is proved, critical values in terms of load can be calculated by comparison of the material properties derived from small scale specimens with the corresponding loading parameters.

Wide plate tests are one possibility of proving the quantitative applicability of fracture mechanics parameters for predicting the failure of large scale samples or components. By Dahl et al. (2) it was demonstrated, that the failure behaviour of

* Institut für Eisenhüttenkunde der Rheinisch-Westfälischen Technischen Hochschule Aachen, Intzestraße 1, D-5100 Aachen.

wide plates with different defect geometries in a temperature range, in which brittle, elastic-plastic and fully plastic failure occurs, can be predicted using a numerical analysis of wide plate tests and the J-integral concept. The procedure of the failure analysis described in detail in (2) is shown schematically in Figure 1. In order to avoid as far as possible any inaccuracy in the failure analysis such as the choice and precision of a plastic limit load equation, the choice of a correct fit of the stress-strain curve of the material by a power law and estimations of the applied loading parameter, finite element (FE) calculations were used to evaluate the fracture mechanics loading conditions.

Nevertheless there exist some problems in predicting failure loads on the applied side - especially for edge cracked panels - as well as on the material side. Therefore the purpose of this paper is to present comparisons between two- and three-dimensional finite element calculations of wide plates and experimental findings by Ehrhardt (3) and to discuss the influence of the choice of the yield criterion and the influence of the strain rate on calculated general-yield loads. Furtheron the influence of different $J_c = J_c(T)$ curves (critical J-integral values as a function of temperature) caused by e.g. different fracture mechanics specimens (size or type, precracked or notched) on the predicted failure loads and on the characteristic transition temperature T_{gy} will be indicated.

DESCRIPTION OF GEOMETRY, MATERIAL AND FE-CALCULATIONS

The geometry in the investigation reported in this paper is a wide plate of DENT-type (double edge notched tension) with width W = 300 mm, thickness B = 30 mm, notch root radius ρ = 0.1 mm and an a/W-ratio of 0.5, see Figure 2a. In the experiments such panels are loaded up to fracture by hydraulic clamping grips with a constant displacement rate of $\dot{v}$ = 2 mm/min. During loading an integral displacement v is measured over a gauge length of L = 360 mm.

In Figure 2b the yield stress R_{eL} of the steel Fe 510 is plotted as a function of temperature. The yielding behaviour was evaluated with smooth tensile specimens at a strain rate of $\dot{\varepsilon} = 8.33 \times 10^{-4}\ s^{-1}$. The approximation of the yield stress with the relation derived on the basis of thermally activated yielding by Krabiell and Dahl (4) enables the calculation of the yield stress for any temperature and strain rate. The wide plate tests were conducted between -70°C and roomtemperature. In this temperature range the yield stress R_{eL} varies between 400 MPa and 470 MPa, whereas the experimentally observed Lueders-strain varies between 1% and 2%.

The computations were performed by the general purpose finite element program ABAQUS by Hibbitt et al. (5) and a modified version of a FE-program, which was originally written by Nayak (6). The uniaxial stress-strain curve was represented by a multilinear approach. Herein the experimentally observed Luedersstrain region was taken into account. For the two- and three-dimensional calculations isoparametric 8-noded and 20-noded elements with reduced integration were used, respectively. The two-dimensional basic mesh (see insert in Figure 3a) represents the result of a convergence study, in which the FE-modelling was investigated in detail. By reason of symmetry conditions only one eighth of the wide plate has to be modelled in the 3-D case. Based on the two-dimensional mesh the finite element structure for the three-dimensional calculation consisting of 3 element layers for half the thickness was generated automatically. Although this division is not necessary for determining the global response of the structure, it was chosen in order to obtain the distribution of the J-integral over the thickness. The J-integral, as introduced by Rice (7) and Cherepanov (8), was calculated using the virtual crack extension technique given by Parks (9). The loading was applied by prescribing displacements at the position of the hydraulic clamping grips.

RESULTS

Subsequently the global response of the wide plate will be discussed in terms of loads, integral displacements and J-integral values. In order to look at the whole temperature range, in which wide plate tests were conducted (see Figure 2b), the comparison between experiments and finite element calculations will be presented in terms of general-yield stresses (external loads at general-yield divided by net cross-section). The influence of different $J_c = J_c(T)$ curves will be demonstrated by comparison of predicted and measured net section stresses.

Global Behaviour

A comparison of two- and three-dimensional computations is shown in Figure 3 by plotting the load as a function of J-integral (a) evaluated as mean value over the thickness in the 3-D case and by plotting the load-displacement curves (b). The plots are normalized using material properties (Young's Modulus E and yield stress R_{el}) and therefore valid for the whole temperature range, but it has to be noticed, that the validity of such a normalization has to be checked. It can be observed, that the plane strain curves are the stiffest ones, as expected, because the plane strain approach doesn't allow a lateral contraction of the geometry. The three-dimensional curves, which must be situated between plane strain and plane stress, are only somewhat stiffer than the plane stress results in the plastic region. Comparing the thickness of the wide plate with the other dimensions this

good agreement could also be expected. Concerning the global behaviour and the application for failure predictions this result indicates, that the plane stress solution is sufficiently precise. The general-yield point determined by plots of the plastic zone was evaluated to 1.16 in the 3-D case, whereas in (1) a factor of $2/\sqrt{3} = 1.155$ is pointed out for plane stress.

Comparison of FE-Calculations with Experiments

Comparing load-displacement curves calculated by FEM with those obtained experimentally over a wide temperature range the extent of quantitative agreement is very different. Qualitatively the curves are similar showing more (experiment) or less (FEM) a distinct yield point because of the Lueders-strain region in the uniaxial stress-strain curve. This characteristic behaviour is responsible for the possibility to determine general-yield loads also from experimental investigations.

Influence of the yield criterion. Summarizing the comparisons of load-displacement curves one can plot the general-yield stress as a function of temperature, see Figure 4. According to Figure 3 the FE-results are situated about 15% (plane stress solution) over the corresponding yield stress R_{eL} determined with smooth tensile specimens and taking into account the strain rate dependence of the yield stress (see equation in Figure 2b). This leads to an overestimation of the general-yield stress from the experiment by the FE-calculation at roomtemperature of about 7%, whereas at -50°C an underestimation of about 4% can be observed. This result can be considered as bad, especially because of the fact, that a tendency can be established and that therefore the results cannot be explained by a scatter effect.

Besides the global behaviour in terms of load-displacement curves there was only one other possibility to compare FE-calculations with experiments, namely the development of the plastic zone. In Figure 5a the experimental findings (3) are shown schematically. One can observe well defined Lueders-lines emanating from the notch root and then spreading out nearly parallel to the ligament up to general-yield load. The FE-result looks quite different, see Figure 5b. Of course, Lueders-lines cannot be obtained from a kontinuumsmechanical model, but also the direction, in which the plastic deformation takes place, is different. In opposite to the experiments the FE-calculation predicts growing of the plastic zone forming an angle of about 45° to the ligament.

Because of these observations the FE-calculation was repeated choosing the yield criterion after TRESCA instead of that after von MISES, which was used in the previous computation. Figure 6 shows a comparison between the MISES- and the TRESCA-results. The shape of the plastic zone using the yield criterion after TRESCA

fits quite good with the experimental one in Figure 5a. Concerning the load-displacement curve one can observe a difference in the plastic region leading to a general-yield point from the TRESCA-result, which is lying about 9% below the MISES one. Summarizing again over a wide temperature range one can plot the temperature dependence of the general-yield stress according to TRESCA in Figure 4. The FE-results are situated about 6% over the yield stress R_{el}. This leads to a quite good description of the experimental results only at higher temperatures, whereas at -50°C an underestimation of the experiment by the FE-calculation of about 11% can be observed. Thus it can be stated, that both solutions, the MISES and the TRESCA one, are not satisfactory.

Influence of the strain rate. Taking into account the better description of the deformation behaviour of the wide plate by the TRESCA-result one has to search for a reason for the large deviations between experiments and FE-solutions at lower temperatures. It is obvious, that higher yield stresses in that region will lead to higher general-yield stresses and thus to a better agreement between experiments and FE-results. The strain rate used in the previous solutions was calculated for the net cross-section of the wide plate assuming elastic deformation only. According to the equation in Figure 2b a higher strain rate will lead to higher yield stresses, especially for lower temperatures. Therefore an attempt was made to evaluate the strain rate from a FE-calculation. Because of the fact, that local values should be obtained, a finer mesh was designed. The number of nodes and elements has been increased by a factor of about 2 as against the previous mesh, but the main difference between the two models is, that the notch root was modelled in detail in the finer mesh.

In Figure 7 the results for the element at the notch root are plotted. Figure 7a shows the time dependence of the strain ε in the ligament ($y \cong 0.0$ mm) and in a distance of about 0.02 mm above the ligament. These curves as well as the "displaced plot" of the mesh, which is inserted, indicate, that the whole deformation takes place in the ligament after a certain time. Figure 7b shows the time dependence of the strain rate $\dot{\varepsilon}$ in the ligament, which was obtained by differentiating the curves out of Figure 7a. The strain rate varies between about $10^{-3}s^{-1}$ and $10^{-1}s^{-1}$.

The influence of the strain rate on the yield stress is demonstrated in Figure 8 by plotting the temperature dependence of the yield stress for four strain rates varying between $10^{-5}s^{-1}$ and $10^{-2}s^{-1}$. Using a strain rate of $10^{-2}s^{-1}$ and the yield criterion after TRESCA this leads to the temperature dependence of the general-yield stress, which is also plotted in Figure 8. One can observe a quite good description of the experimental results by the FE-calculation over the whole temperature range. All

the points are lying in a scatter band, which is smaller than 5%, and - what is more important - in opposite to the previous solutions no tendency can be established concerning the deviations. The result of this detailed study gives an impression of the order of magnitude of the strain rate, which occurs locally, but it is not easy to deduct to what extent the yield stresses following from the high strain rate are relevant for the global behaviour of the wide plate. Because of the fact, that a global assumption of the strain rate based on plastic deformation also leads to higher values than assuming elastic deformation only, it can be argued, that the strain rate calculated by using the overall length, is too low.

Influence of the Geometry Dependence of Fracture Mechanics Properties on the Failure Prediction

As mentioned before and indicated in Figure 1 the predicted failure loads do not depend only on the fracture mechanics loading parameters, but also on their critical material properties. The problems on the applied side were discussed above in detail. Subsequently an impression shall be given how far the failure prediction is influenced by different $J_c = J_c(T)$ curves.

The critical values of the J-integral were determined using 13 mm thick 1CT-specimens (1CT-13) according to Merkle and Corten (10). The onset of stable crack growth was observed at a temperature of -20°C, so that below this temperature J_c-values were determined for specimens failed in an unstable manner. Above this temperature J_{Ic} characterizes the onset of stable crack growth. The J_{Ic}-values, being independent of temperature, were determined from J_R-curves to $J_{Ic} = 220$ N/mm. All these data together lead to curve 1 in Figure 9, which represents the input curve for the failure analysis from the material side. The result of the failure analysis using this curve and taking into account the consequences from the discussion of the applied side (TRESCA, $\dot{\varepsilon} = 10^{-2}\,s^{-1}$) is shown in Figure 10 (curve 1). The comparison between predicted and experimentally determined net section stresses demonstrates the possibility of a quantitative failure prediction based on J_c and J_{Ic}. The characteristic temperature T_{qv} of the wide plates correlates quite well with the calculated transition temperature. Due to the improvements on the applied side the quantitative agreement over the whole temperature range is better than in a previous paper (2), in which a more detailed discussion is given including an analysis based on J_R-curve.

The results of a lot of experimental work (see e.g. Sun et al. (11), Heuser and Dahl (12)) demonstrate, that the fracture mechanics properties for the onset of stable crack growth (J_{Ic}) as well as for the crack resistance behaviour (J_R-curve), which shall be used for a safety analysis, are dependent on the specimen geometry (size, type, side-grooving). Besides that a shift

in transition temperature of about 30°C was observed by Schmitz-Cohnen (13), if side-grooved 3-point bend specimens are fractured instead of non side-grooved specimens. Testing wide plates of CNT-type (center notched tension) instead of those containing fatigue cracks also leads to a shift in transition temperature, see Rosezin (14).

Therefore besides the measured critical values of the J-integral two kinds of fictitious data were used for the failure analysis. Concerning the geometry dependence of J_{Ic} nearly no influence on the predicted net section stresses could be observed for the DENT-plate with a/W = 0.5. The second kind of fictitious data represents a shift in transition temperature and is plotted in Figure 9 (curve 2). The result of the failure analysis using this curve is shown in Figure 10 (curve 2). As expected, one can observe a shift in transition temperature for the wide plates, too, and that leading to a worse description of the experimental values by the failure analysis.

Summarizing the results of the material side concerning the failure analysis one can state, that the main problem is to decide, which critical values of the J-integral or of another fracture mechanics parameter are valid for a certain structural component and therefore relevant for a failure assessment of this component.

SUMMARY AND CONCLUSIONS

A plane stress solution is sufficiently precise for determining the global response of the investigated DENT-plate and also for its application for failure predictions using the J-integral concept.

Using the yield criterion after von MISES does not lead to satisfying results. The deformation behaviour of the wide plate is described better by the yield criterion after TRESCA. Of course, that means, that the FE-program must contain the yield criterion after TRESCA, and this is not self-evident for the commercially available codes.

Because of the strain rate dependence of the yield stress the determination of the strain rate becomes important with decreasing temperature. The strain rates at the notch root are higher than those from the smooth tensile specimens by a factor of about 100.

On the material side the crucial point for a failure assessment of a structural component is the question, what kind of fracture mechanics specimen has to be tested in order to obtain critical values, which are responsible for the failure behaviour of the component, too.

REFERENCES

(1) Kumar, V., German, M.D. and Shih, C.F., "An Engineering Approach for Elastic-Plastic Fracture Analysis", EPRI, Palo Alto, U.S.A., Report No. NP-1931, 1981.

(2) Dahl, W., Dormagen, D., Ehrhardt, H., Hesse, W. and Twickler, R., Nucl. Engng & Des., Vol. 87, 1985, pp. 83-88.

(3) Ehrhardt, H., work in progress.

(4) Krabiell, A. and Dahl, W., Arch. Eisenhüttenwes., Vol. 52, No. 11, 1981, pp. 429-436.

(5) Hibbitt, H.D., Karlsson, B.I. and Sorensen, P., HKS Inc., Providence R.I., U.S.A., ABAQUS User's Manual, Version 4.5, 1984.

(6) Nayak, G.C., "Plasticity and large deformation by the finite element method", Ph.D. dissertation, University of Wales, 1971.

(7) Rice, J.R., J. Appl. Mech., Vol. 35, 1968, pp. 379-386.

(8) Cherepanov, G.P., J. Appl. Math. Mech., Vol. 31, 1967, pp. 503-512.

(9) Parks, D.M., Comp. Meths. Appl. Mech. Engng, Vol. 12, 1977, pp. 353-364.

(10) Merkle, J.G. and Corten, H.T., Trans. ASME, J. Pres. Ves. Techn., Vol. 96, 1974, pp. 286-292.

(11) Sun, D.Z., Dormagen, D. and Dahl, W., steel research, Vol. 56, No. 8, 1985, pp. 445-449.

(12) Heuser, A. and Dahl, W., Materialprüf., Vol. 26, No. 11, 1984, pp. 389-393.

(13) Schmitz-Cohnen, K., private communication.

(14) Rosezin, H.J., "Beurteilung des Bruchverhaltens von Stählen auf der Grundlage von Großzugversuchen", Ph.D. dissertation, RWTH Aachen, FRG, 1983.

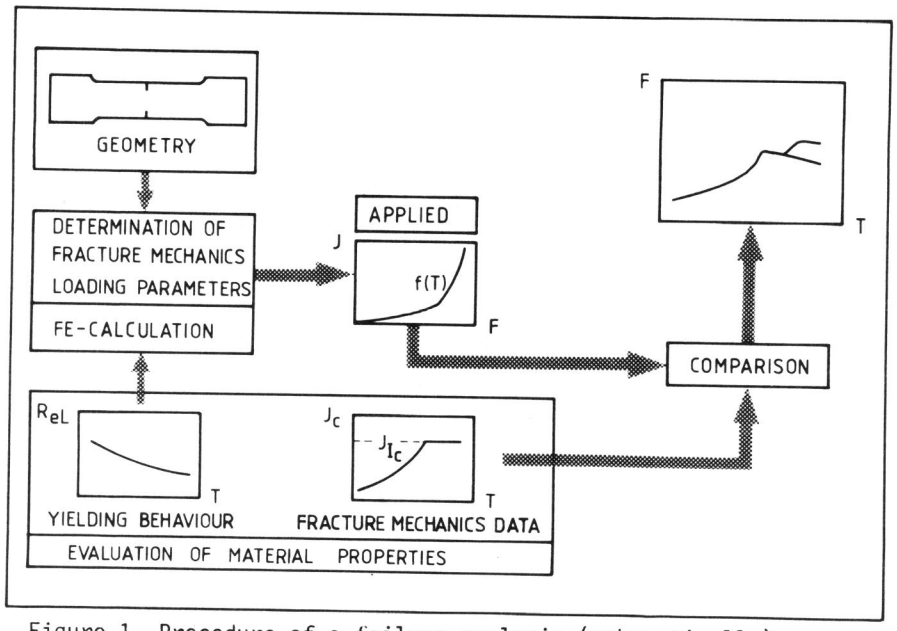

Figure 1. Procedure of a failure analysis (schematically)

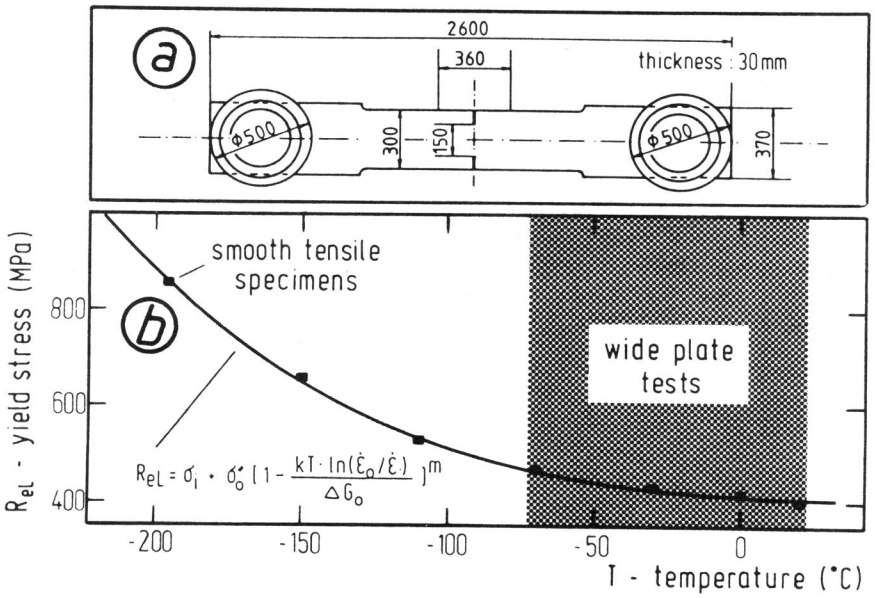

Figure 2. Investigated geometry (a) and yield stress R_{eL} of Fe 510 steel as a function of temperature (b)

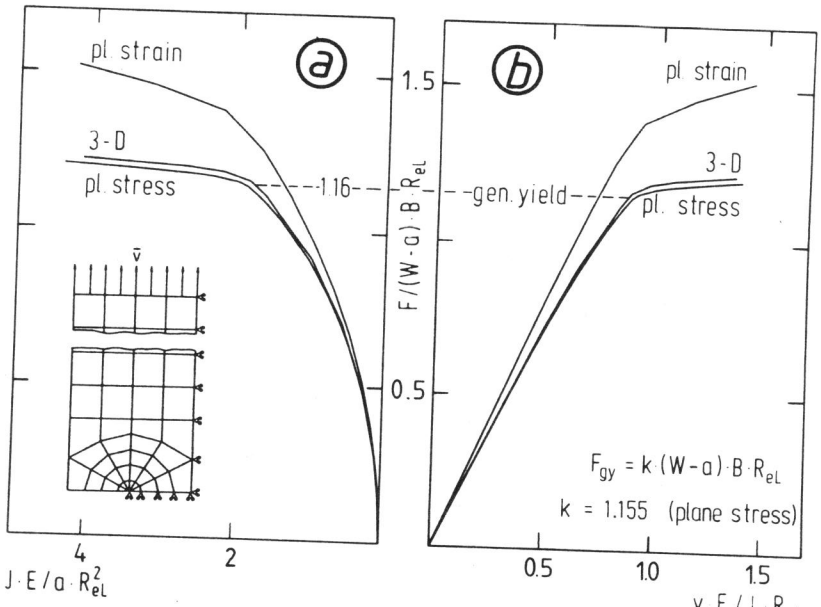

Figure 3. Comparison of 2- and 3-D FE-computations: load vs J-integral (a) and load-displacement curves (b), both normalized

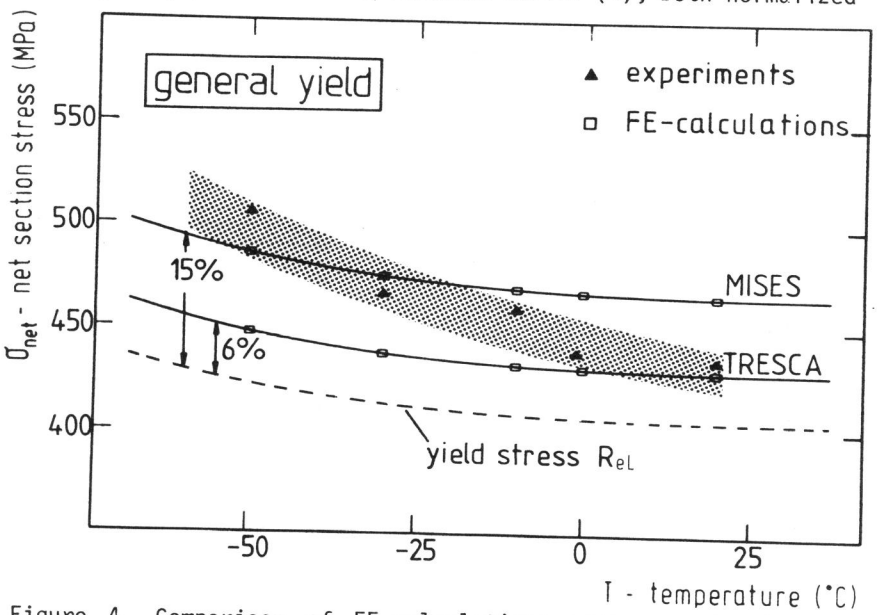

Figure 4. Comparison of FE-calculations with experiments: net section stresses at general-yield as a function of temperature

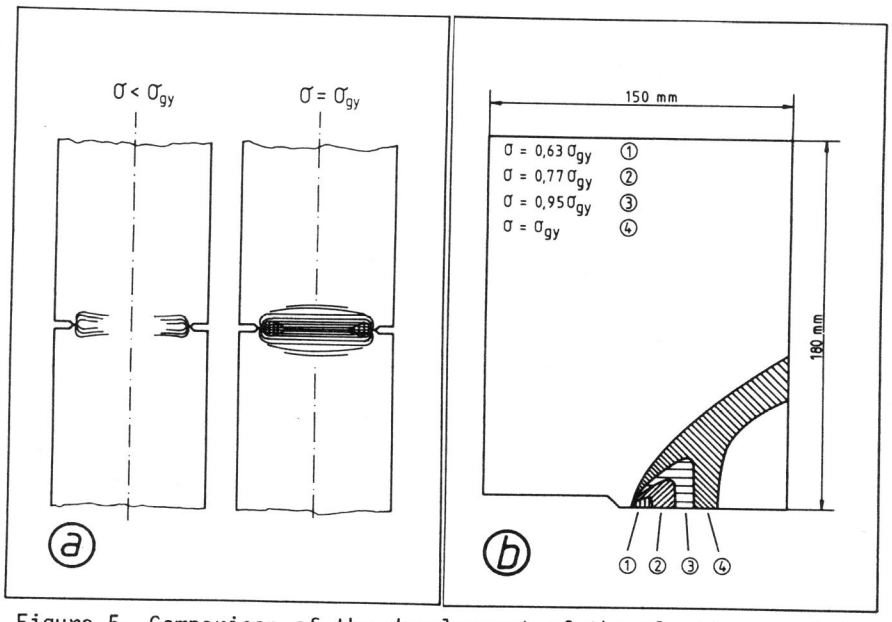

Figure 5. Comparison of the development of the plastic zone between experimental findings (a) and the FE-result (b)

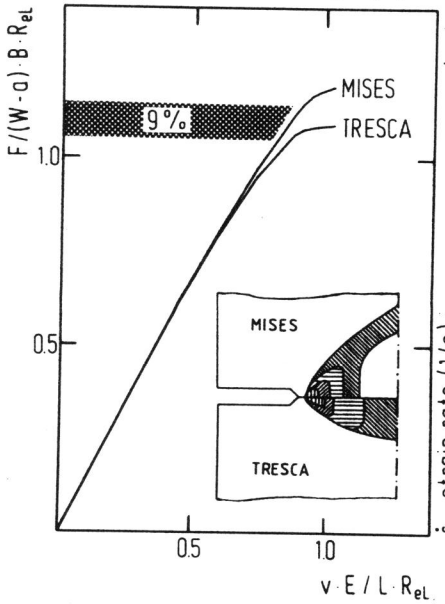

Figure 6. Comparison of MISES- and TRESCA-results

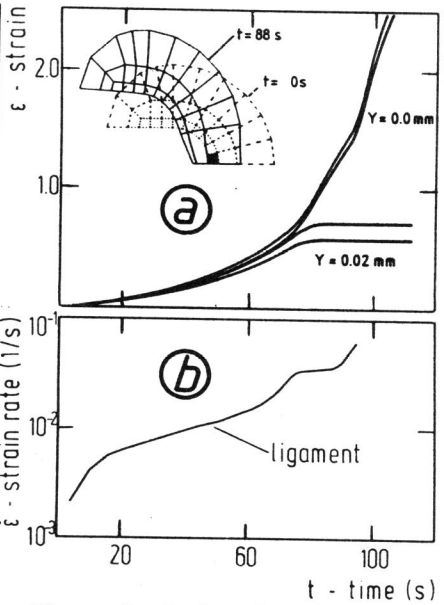

Figure 7. Evaluation of strain rates

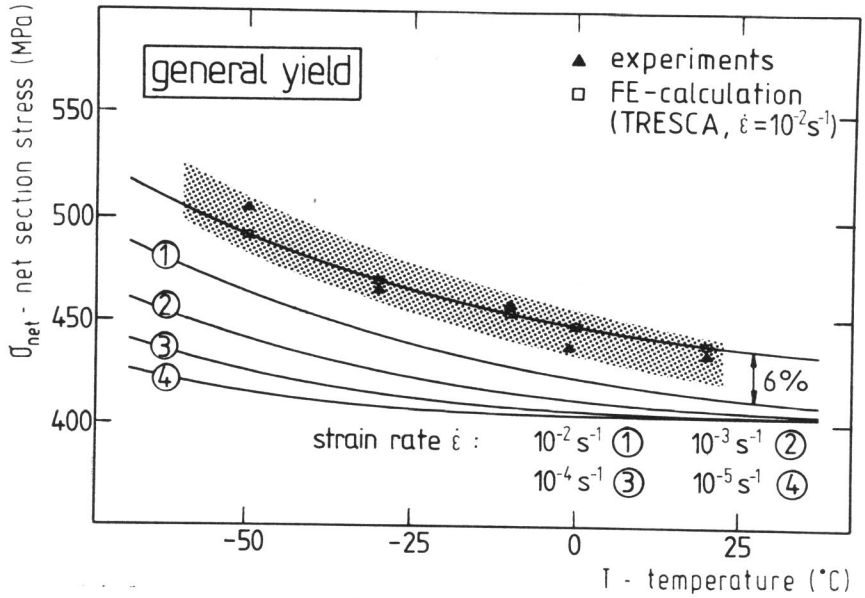

Figure 8. Influence of the strain rate on the yield stress and comparison of FE-solutions with experiments at general-yield

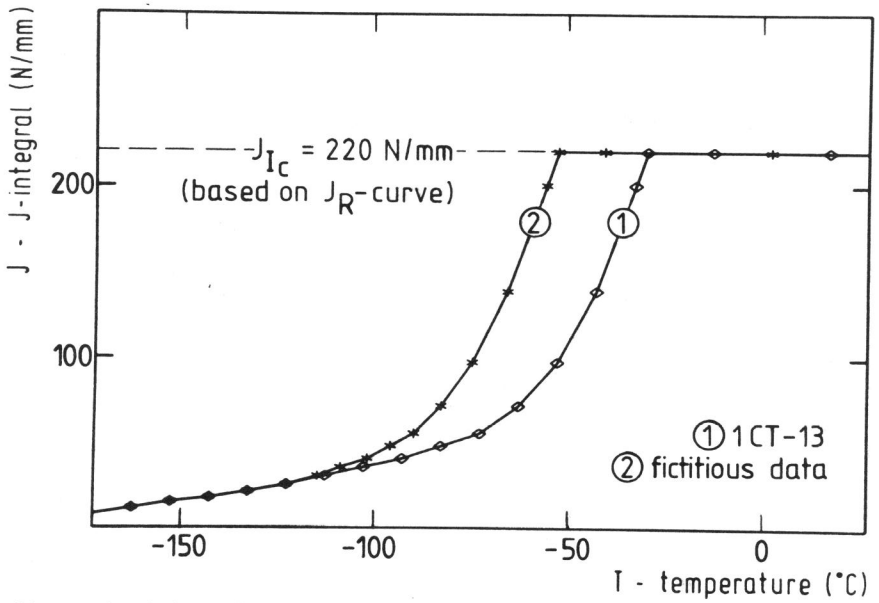

Figure 9. Critical J-integral values as a function of temperature for Fe 510 steel

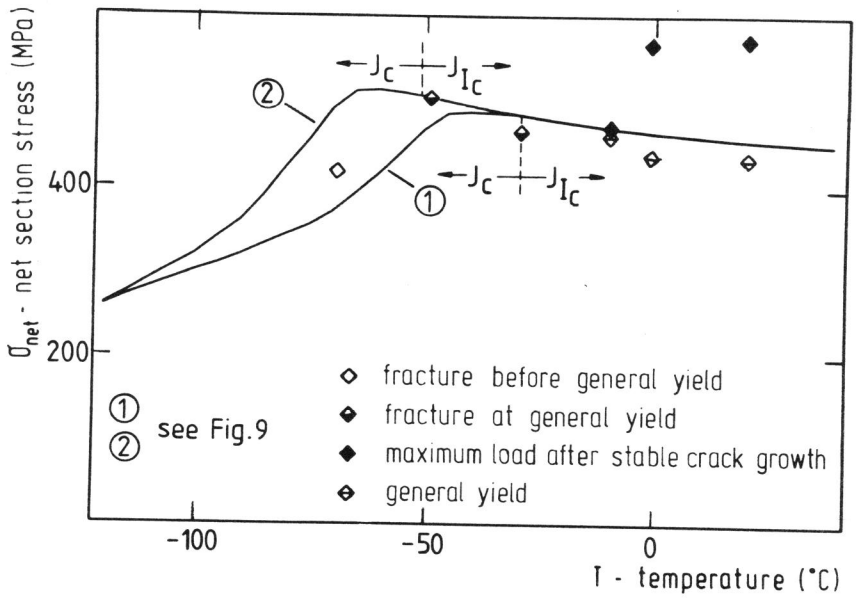

Figure 10. Influence of different $J_c = J_c(T)$ curves on the failure prediction